ECOs from the dark DM cores

Presenters: Jingfeng Pan, Katie Tamura, Udhay Dogra

Tutors: Laura Sagunski, Robin Diedrichs

Outlines

1. Introduction
   - Gravitational waves from merging black holes and neutron stars (three phases of the merger)
   - Mention LIGO detections
   - Peaks in the power spectral density (PSD) for a neutron star merger
   - Neutron stars with dark matter cores
2. Theoretical model
   - Toy model from Ellis et. al
   - Derivation of the PSD:
     i. Equations of motion
     ii. Quadrupole moment
   - Plots for the Gravitational wave signal
   - Plot for the PSD
3. Numerical results
   - Our plots h+ and hx in comparison to Ellis et al.
   - Our plots for the PSD for different values of the free parameters
4. Conclusions and outlook
   - Summary
   - Open problems: Cannot reproduce oscillations in the PSD that Ellis et al. have
   - Realistic values for the free parameters, e.g., the dark matter mass fraction (see https://arxiv.org/abs/2303.04089)

1. Introduction

Stages of Binary BH/NS Mergers

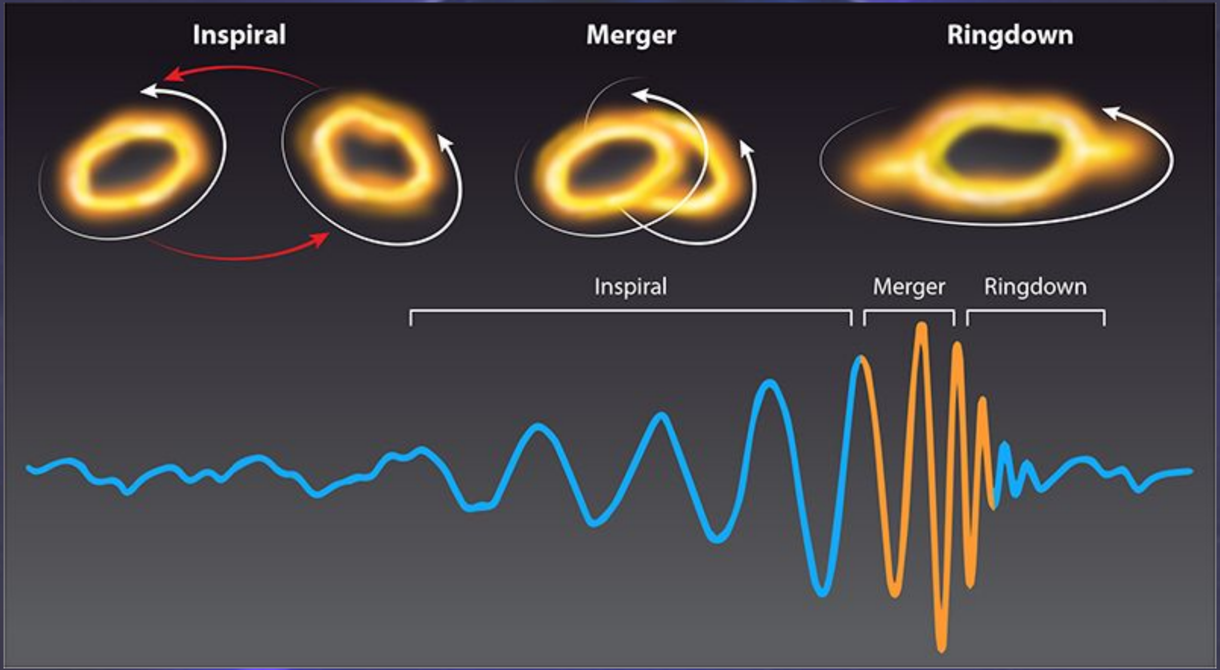

Credit :(Top) Kip Thorne; (Bottom) B. P. Abbott et al. [8]; adapted by APS/Carin Cain
https://physics.aps.org/articles/v16/29

LIGO Detections

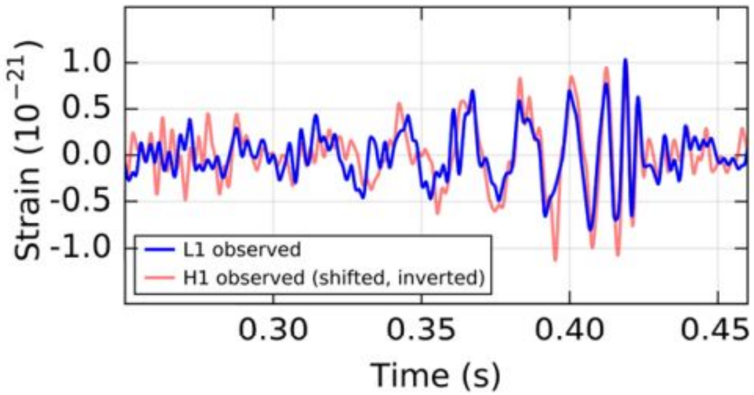

Figure 1 The instrumental strain data in the Livingston detector (blue) and Hanford detector (red), as shown in Figure 1 of [1]. Both have been bandpass- and notch-filtered. The Hanford strain has been shifted back in time by 6.9 ms and inverted. Times shown are relative to 09:50:45 Coordinated Universal Time (UTC) on September 14, 2015.

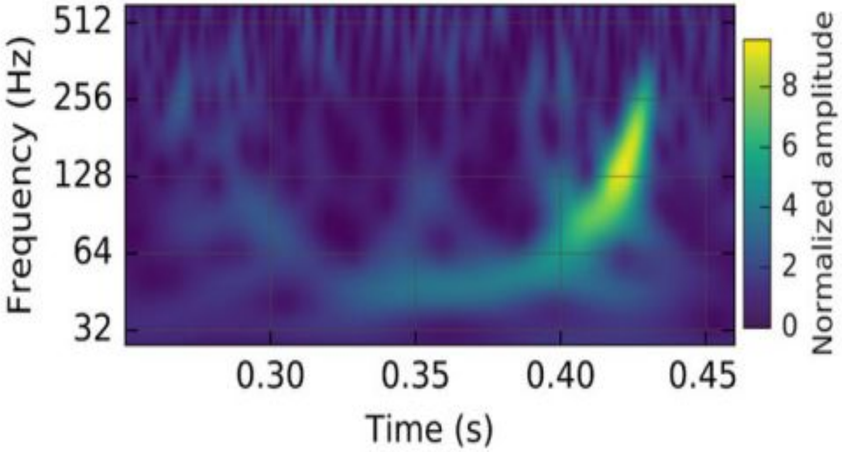

Figure 2 A representation of the strain-data as a time-frequency plot (taken from [1]), where the increase in signal frequency ("chirp") can be traced over time.

Credit: Abbot et al. [1]

PSD for a NS Post-Merger

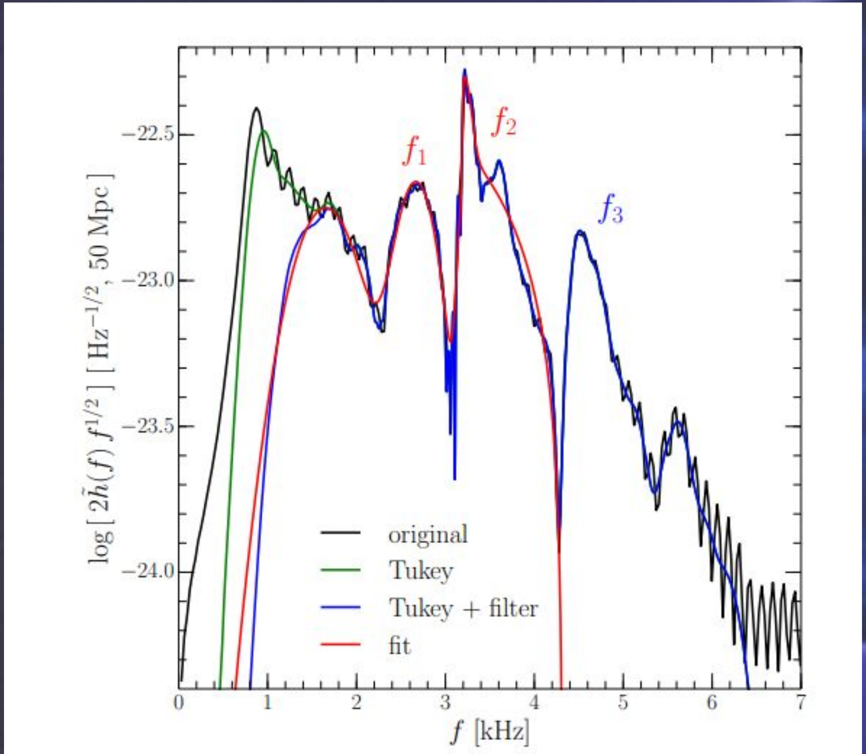

FIG. 3. PSD $2\tilde{h}(f)f^{1/2}$ relative to the binary `APR4-q10-M1375`. Indicated with a black line is the full PSD, while the green line shows the PSD after the application of a Tukey window, and the blue line the PSD filtered with a high-pass Butterworth filter. Finally, shown in red is the fit made to capture the peak frequencies f_1 and f_2.

Credit: Takami et al. [2]

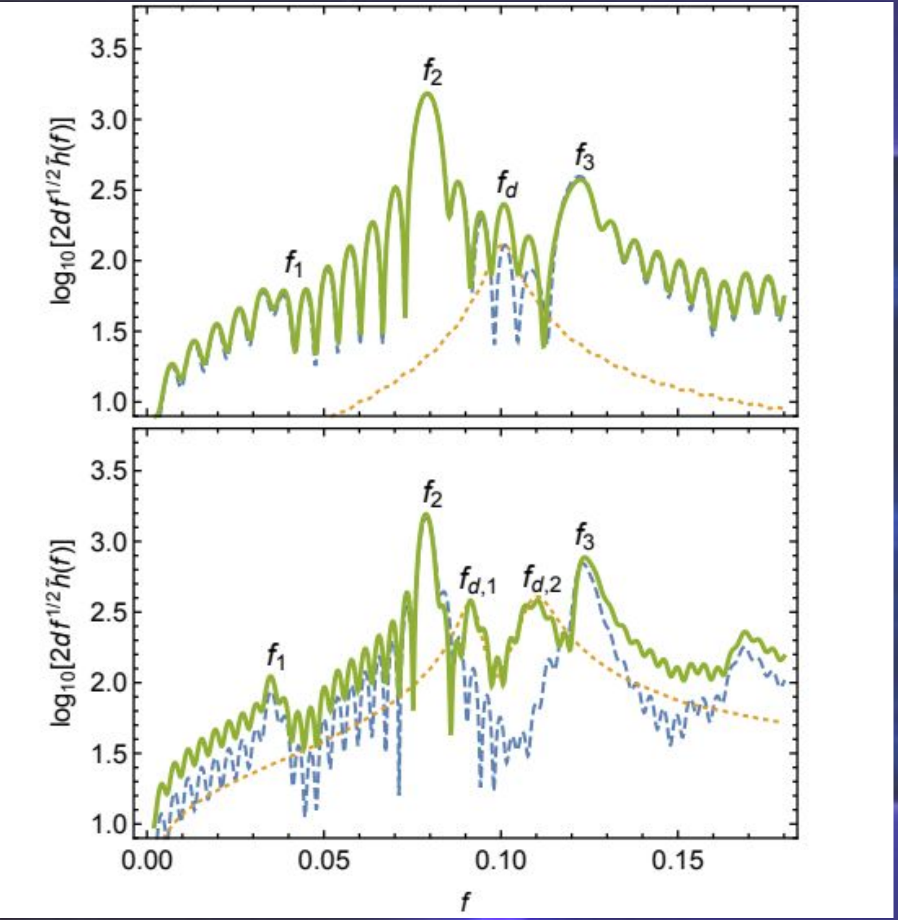

Credit: Ellis et al. [2]

Adding Dark Matter Cores

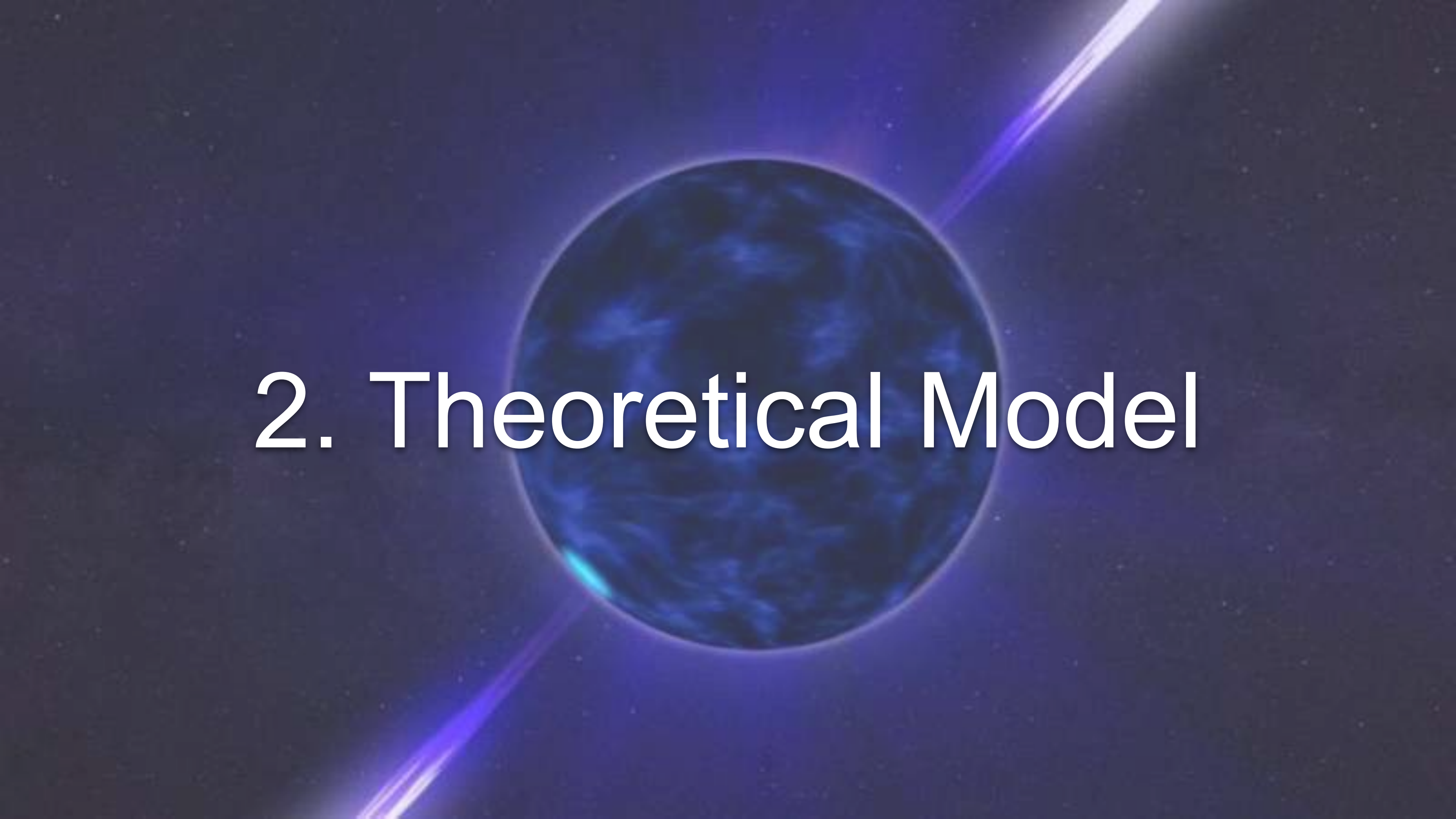

2. Theoretical Model

Toy Model

Original Toy Model

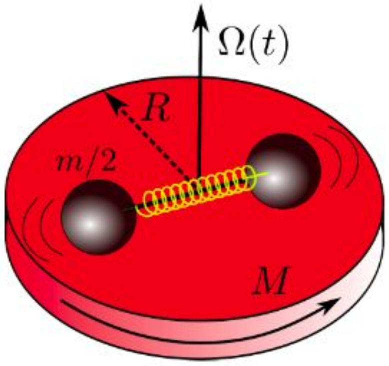

FIG. 17. Cartoon of the mechanical toy model composed of a disk of mass M and radius R rotating at frequency $\Omega(t)$. Two spheres, each of mass $m/2$ are connected to the disk, but are also free to oscillate via a spring that connects them.

Takami et. al [2]

Extended Toy Model

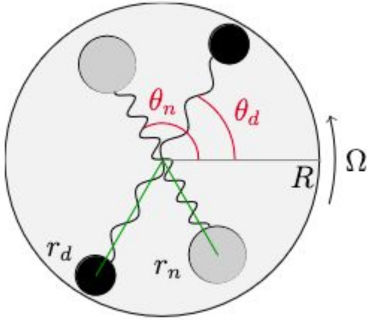

FIG. 1. A schematic diagram of the mechanical model adopted to investigate the possible effects of DM components on the GW signal emitted by NS-NS mergers. The DM cores (in black) move in an environment constituted of the remnant neutron stellar core (in white) and a disk of neutron matter enclosing the latter.

Ellis et. al [3]

Derivation of Equations of Motion

$$\frac{\mathrm{d}}{\mathrm{d}t}\frac{\partial L}{\partial \dot{q}_j} - \frac{\partial L}{\partial q_j} = \frac{\partial D}{\partial \dot{q}_j}\,. \qquad (3)$$

$$L = \frac{m_n}{2}\left(\dot{r}_n^2 + \left(r_n\dot{\theta}_n\right)^2\right) + \frac{m_d}{2}\left(\dot{r}_d^2 + \left(r_d\dot{\theta}_d\right)^2\right) + \frac{MR^2\dot{\theta}_n^2}{4} + 2k_n(r_n - a_n)^2 + 2k_d(r_d - a_d)^2\,, \qquad (1)$$

$$D = -\,b_n\dot{r}_n^2 - b_d\left(\dot{r}_d^2 + \left(r_d\left(\dot{\theta}_n - \dot{\theta}_d\right)\right)^2\right) - c_n\left(\dot{r}_n^2 + \left(r_n\dot{\theta}_n\right)^2\right) - c_d\left(\dot{r}_d^2 + \left(r_d\dot{\theta}_d\right)^2\right)\,. \qquad (2)$$

Ellis et. al [3]

For r_n and $\dot{r}_n$:

$$m_n\ddot{r}_n + 2(b_n + c_n)\dot{r}_n - \left(m_n\dot{\theta}_n^2 + 4k_n\right)r_n + 4k_n a_n = 0$$

For θ_n and $\dot{\theta}_n$:

$$\left(m_n r_n^2 + \frac{1}{2}MR^2\right)\ddot{\theta}_n + 2(m_n r_n\dot{r}_n + b_d r_d^2 + c_n r_n^2)\dot{\theta}_n - 2b_d r_d^2\dot{\theta}_n = 0$$

For r_d and $\dot{r}_d$:

$$m_d\ddot{r}_d + \left[2(b_d + c_d) - m_d\dot{\theta}_d^2 - 4k_d\right]r_d + 4k_d a_d = 0$$

For θ_d and $\dot{\theta}_d$:

$$m_d r_d^2\ddot{\theta}_d + 2[m_d r_d\dot{r}_d + r_d^2(b_d + c_d)]\dot{\theta}_d - 2b_d r_d^2\dot{\theta}_n = 0$$

Solutions of equation (3)

Derivation of Equations of Motion

$$\frac{\mathrm{d}}{\mathrm{d}t}\frac{\partial L}{\partial \dot{q}_j} - \frac{\partial L}{\partial q_j} = \frac{\partial D}{\partial \dot{q}_j}\,. \qquad (3)$$

Ellis et. al [3]

Code for equation (3)

```python
def fun(t, y):
    rn = y[0]
    thetan = y[1]
    rn_dot = y[2]
    thetan_dot = y[3]

    rd = y[4]
    thetad = y[5]
    rd_dot = y[6]
    thetad_dot = y[7]

    rn_dotdot = 1/mn * (mn * thetan_dot**2 * rn - 4 * kn * (rn - an) - 2 * (bn + cn) * rn_dot)
    rd_dotdot = 1/md * (md * thetad_dot**2 * rd - 4 * kd * (rd - ad) - 2 * (bd + cd) * rd_dot)

    thetan_dotdot = 1/(mn * rn**2 + M * R**2 / 2) * (-2 * mn * rn * rn_dot * thetan_dot - 2 * (bd * rd**2 + cn * rn**2) * thetan_dot + 2 * bd * rd**2 * thetad_dot)
    thetad_dotdot = 1/(md * rd**2) * (-2 * (md * rd * rd_dot + bd * rd**2 + cd * rd**2) * thetad_dot - 2 * bd * rd**2 * thetan_dot)

    return [rn_dot, thetan_dot, rn_dotdot, thetan_dotdot, rd_dot, thetad_dot, rd_dotdot, thetad_dotdot]

y0 = [initialConditions.rn, initialConditions.thetan, initialConditions.rn_dot, initialConditions.thetan_dot,
      initialConditions.rd, initialConditions.thetad, initialConditions.rd_dot, initialConditions.thetad_dot]

sol = solve_ivp(fun, [0, tmax], y0=y0, max_step=dt, rtol=1, atol=1)
```

Derivation of Quadrupole Moment

$$h_+ = \frac{\ddot{I}_{xx} + \ddot{I}_{yy}}{D}, \quad h_\times = \frac{\ddot{I}_{xy}}{D}, \tag{4}$$

$$I_{kl} = \sum_{j=n,d} \left(\bar{I}_{j,kl} - \frac{1}{3}\delta_{kl}\delta^{ab}\bar{I}_{j,ab} \right), \tag{5}$$
$$\bar{I}_{j,kl} = 3m_j x_{j,k} x_{j,l}.$$

Ellis et. al [3]

$$\delta^{ab}\bar{I}_{j,ab} \equiv \sum_{a=1}^{3}\sum_{b=1}^{3} \delta^{ab}\bar{I}_{j,ab}$$

Einstein sum notation

$$\delta^{00} = 1, \delta^{01} = 0$$

Kronecker delta

Solutions of equation (5)

$$\begin{aligned}\ddot{I}_{xx} = {} & 2m_n(\dot{r}_n^2 + r_n\ddot{r}_n)(2cos^2\theta_n - sin^2\theta_n) - 12m_n r_n\dot{r}_n sin2\theta_n\dot{\theta}_n \\ & + 3m_n r_n^2(2cos2\theta_n\dot{\theta}_n + sin2\theta_n\ddot{\theta}_n) + 2m_d(\dot{r}_d^2 + r_d\ddot{r}_d)(2cos^2\theta_d - sin^2\theta_d) \\ & - 12m_d r_d\dot{r}_d sin2\theta_d\dot{\theta}_d + 3m_d r_d^2(2cos2\theta_d\dot{\theta}_d + sin2\theta_d\ddot{\theta}_d)\end{aligned}$$

$$\begin{aligned}\ddot{I}_{yy} = {} & 2m_n(\dot{r}_n^2 + r_n\ddot{r}_n)(2cos^2\theta_n - sin^2\theta_n) + 12m_n r_n\dot{r}_n sin2\theta_n\dot{\theta}_n \\ & + 3m_n r_n^2(2cos2\theta_n\dot{\theta}_n + sin2\theta_n\ddot{\theta}_n) + 2m_d(\dot{r}_d^2 + r_d\ddot{r}_d)(2cos^2\theta_d - sin^2\theta_d) \\ & + 12m_d r_d\dot{r}_d sin2\theta_d\dot{\theta}_d + 3m_d r_d^2(2cos2\theta_d\dot{\theta}_d + sin2\theta_d\ddot{\theta}_d)\end{aligned}$$

$$\begin{aligned}\ddot{I}_{xy} = {} & 3m_n[(\dot{r}_n^2 + r_n\ddot{r}_n)sin2\theta_n + 4r_n\dot{r}_n cos2\theta_n\dot{\theta}_n + r_n^2(-2sin2\theta_n\dot{\theta}_n + cos2\theta_n\ddot{\theta}_n)] \\ & + 3m_d[(\dot{r}_d^2 + r_d\ddot{r}_d)sin2\theta_d + 4r_d\dot{r}_d cos2\theta_d\dot{\theta}_d + r_d^2(-2sin2\theta_d\dot{\theta}_d + cos2\theta_d\ddot{\theta}_d)]\end{aligned}$$

Derivation of Quadrupole Moment

$$I_{kl} = \sum_{j=n,d} \left(\bar{I}_{j,kl} - \frac{1}{3}\delta_{kl}\delta^{ab}\bar{I}_{j,ab} \right) , \qquad (5)$$

$$\bar{I}_{j,kl} = 3 m_j x_{j,k} x_{j,l} \, .$$

Ellis et. al [3]

Code for equation (5)

```
Ixx_2dots = 2*mn*(rnDotVals**2 + rnVals*rn2dotsVals)*(2*np.cos(thetanVals)**2 - np.sin(thetanVals)**2) \
            - 12*mn*rnVals*rnDotVals*np.sin(2*thetanVals)*thetanDotVals \
            + 3*mn*(rnVals**2)*(2*np.cos(2*thetanVals)*thetanDotVals + np.sin(2*thetanVals)*thetan2dotsVals) \
            + 2*md*(rdDotVals**2 + rdVals*rd2dotsVals)*(2*np.cos(thetadVals)**2 - np.sin(thetadVals)**2) \
            - 12*md*rdVals*rdDotVals*np.sin(2*thetadVals)*thetadDotVals \
            + 3*md*(rdVals**2)*(2*np.cos(2*thetadVals)*thetadDotVals + np.sin(2*thetadVals)*thetad2dotsVals)

Iyy_2dots = 2*mn*(rnDotVals**2 + rnVals*rn2dotsVals)*(2*np.sin(thetanVals)**2 - np.cos(thetanVals)**2) \
            + 12*mn*rnVals*rnDotVals*np.sin(2*thetanVals)*thetanDotVals \
            + 3*mn*(rnVals**2)*(2*np.cos(2*thetanVals)*thetanDotVals + np.sin(2*thetanVals)*thetan2dotsVals) \
            + 2*md*(rdDotVals**2 + rdVals*rd2dotsVals)*(2*np.sin(thetadVals)**2 - np.cos(thetadVals)**2) \
            + 12*md*rdVals*rdDotVals*np.sin(2*thetadVals)*thetadDotVals \
            + 3*md*(rdVals**2)*(2*np.cos(2*thetadVals)*thetadDotVals + np.sin(2*thetadVals)*thetad2dotsVals)

Ixy_2dots = 3*mn*((rnDotVals**2 + rnVals*rn2dotsVals)*np.sin(2*thetanVals) + 4*rnVals*rnDotVals*np.cos(2*thetanVals)*thetanDotVals
            + rnVals**2*(-2*np.sin(2*thetanVals)*thetanDotVals + np.cos(2*thetanVals)*thetan2dotsVals)) \
            + 3*md*((rdDotVals**2 + rdVals*rd2dotsVals)*np.sin(2*thetadVals) + 4*rdVals*rdDotVals*np.cos(2*thetadVals)*thetadDotVals
            + rdVals**2*(-2*np.sin(2*thetadVals)*thetadDotVals + np.cos(2*thetadVals)*thetad2dotsVals))
```

Plots for the Gravitational Wave Signal

$$h_+ = \frac{\ddot{I}_{xx} + \ddot{I}_{yy}}{D}, \quad h_\times = \frac{\ddot{I}_{xy}}{D}, \tag{4}$$

Ellis et. al [3]

Plots for the
h+ and hx

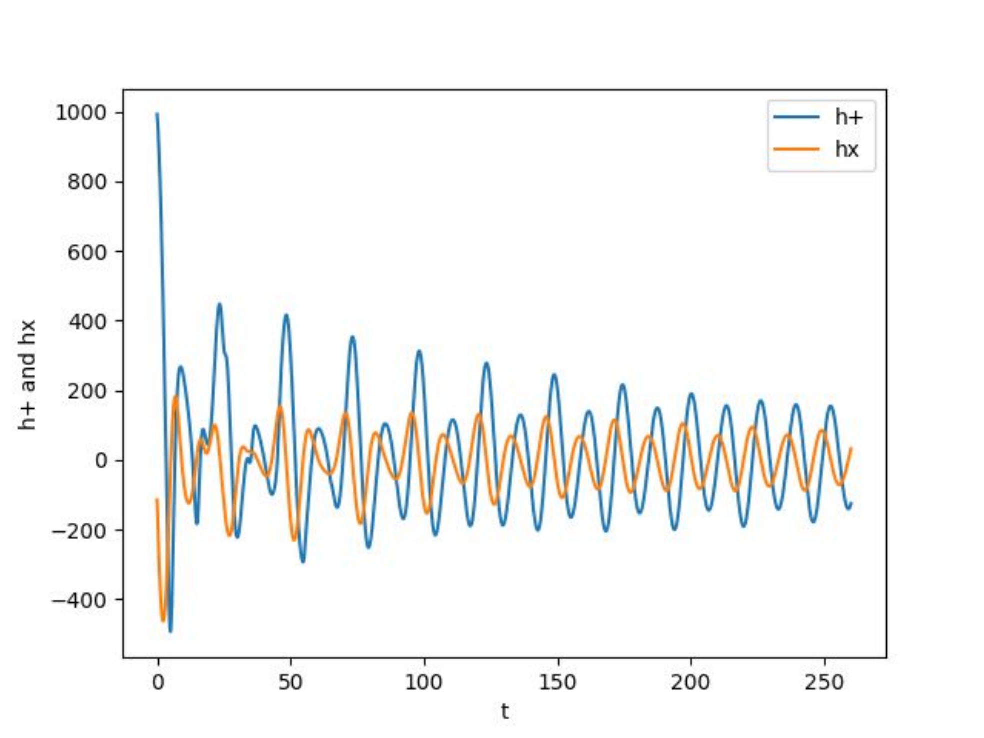

Plot for the PSD

$$\tilde{h}(f) = \sqrt{\frac{|\tilde{h}_+(f)|^2 + |\tilde{h}_\times(f)|^2}{2}}, \tag{6}$$

Ellis et. al [3]

Plot for the PSD

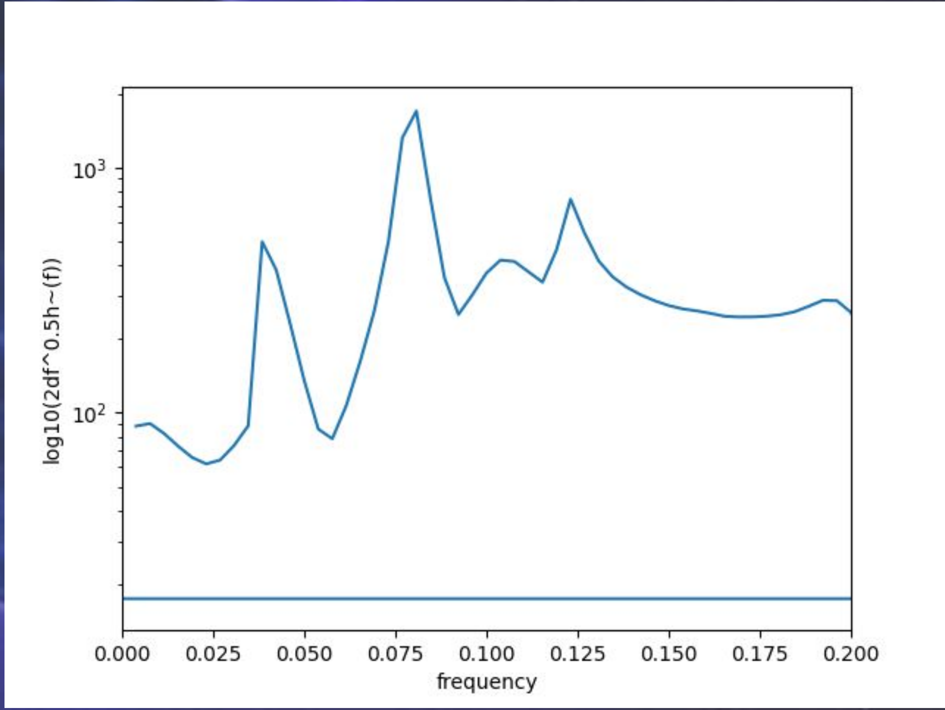

3. Numerical Results

Plots of H_+

Ellis et al.

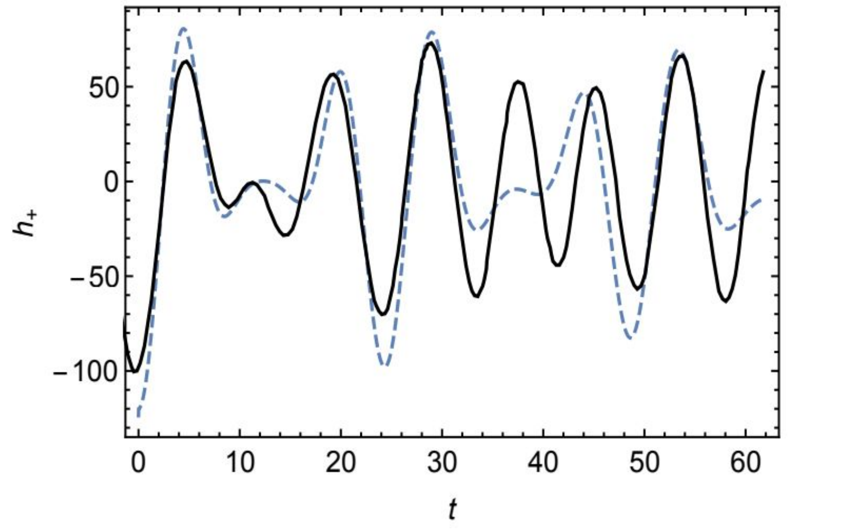

EXPLORE Team

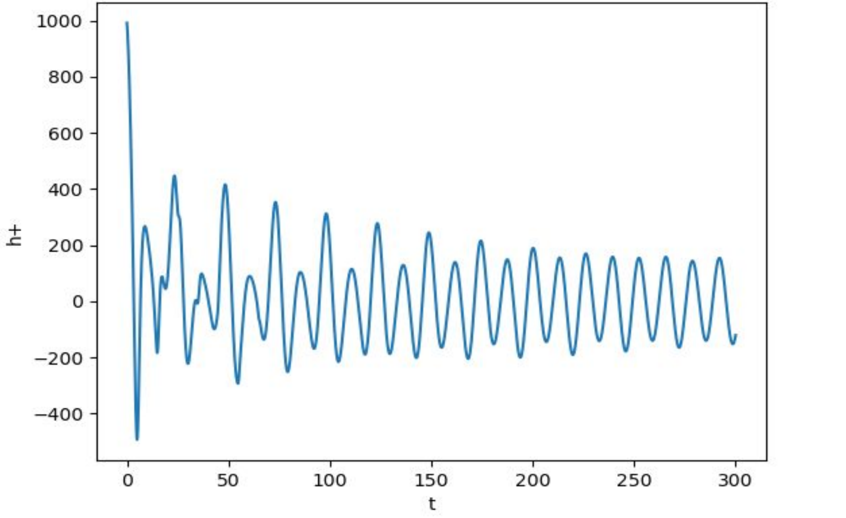

PSD Plots

Ellis et al.

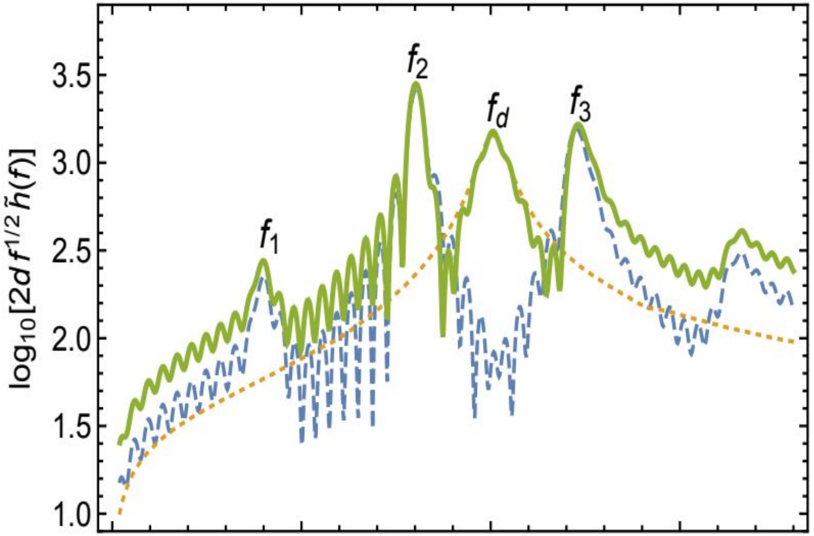

EXPLORE Team

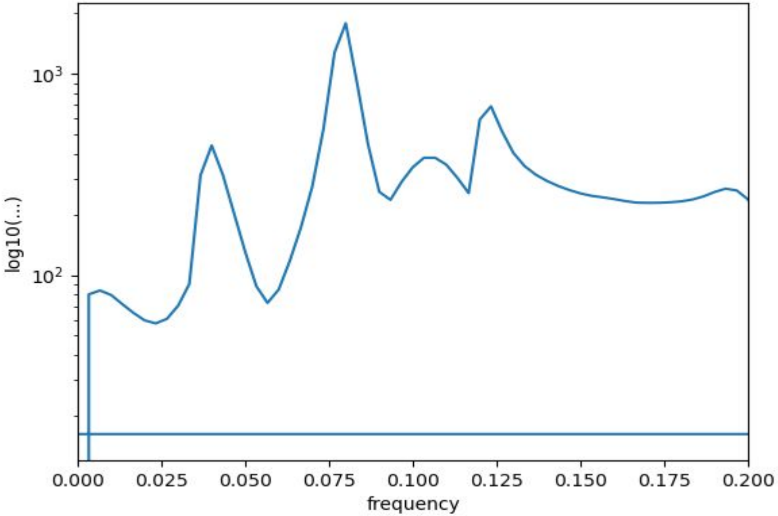

Change of Radius ($R_{initial}$=10)

Change of θ ($θ_{initial}$=0.2)

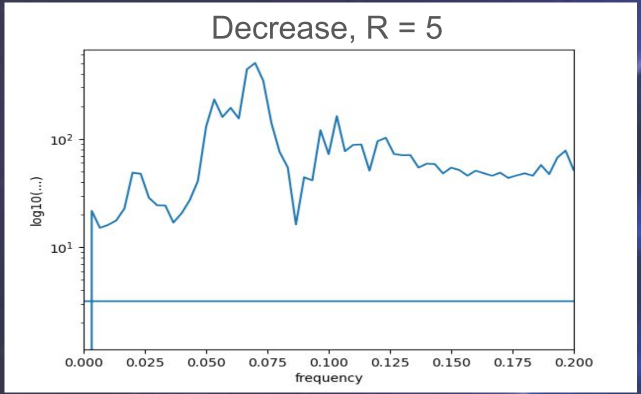

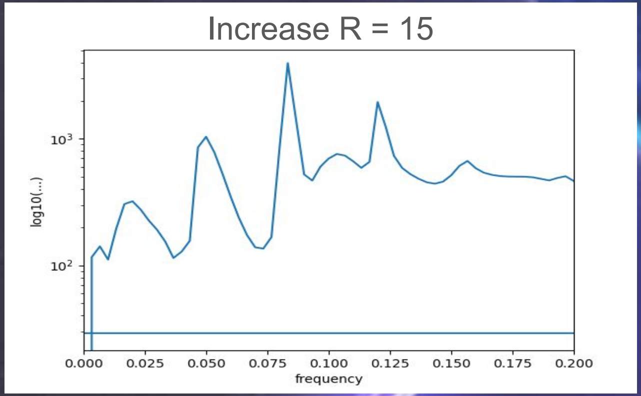

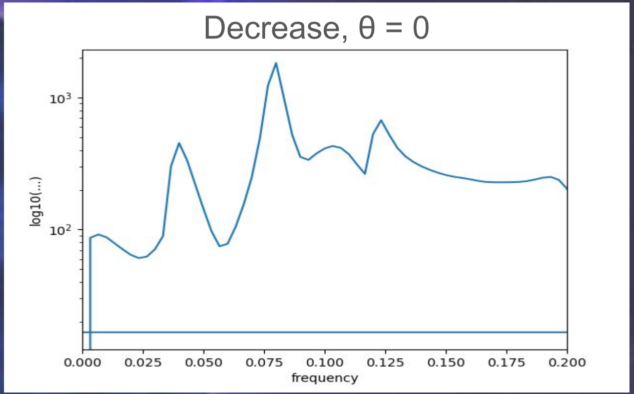

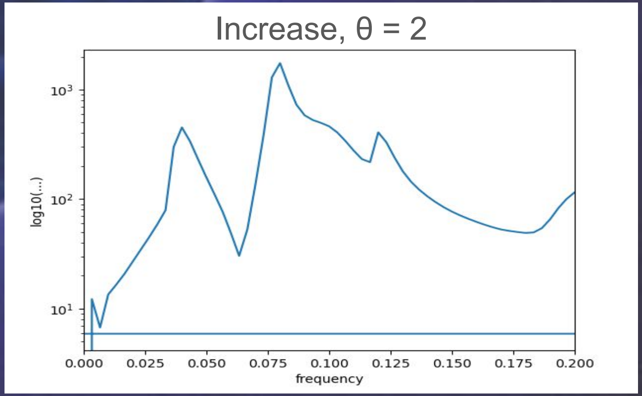

Change of dt ($dt_{initial}$=0.02)

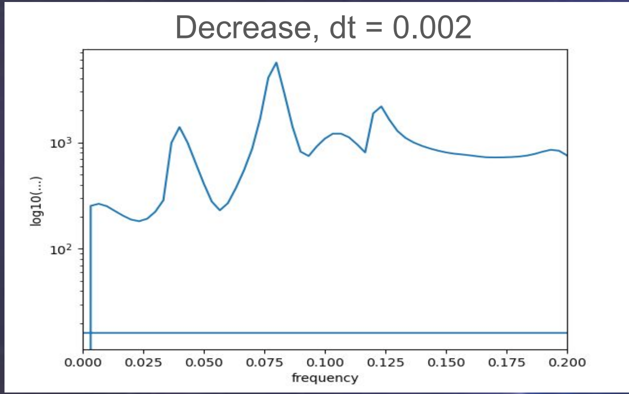

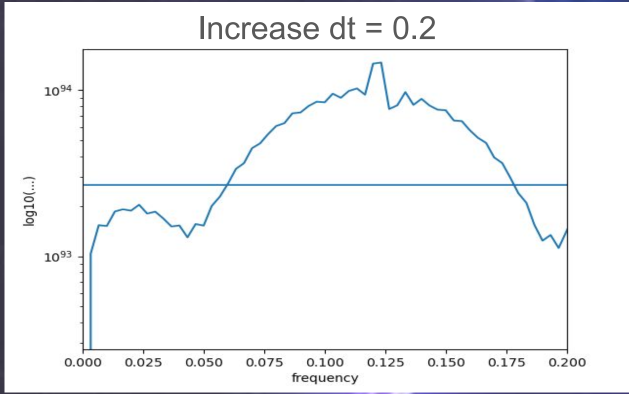

Change of tmax ($tmax_{initial}$=300)

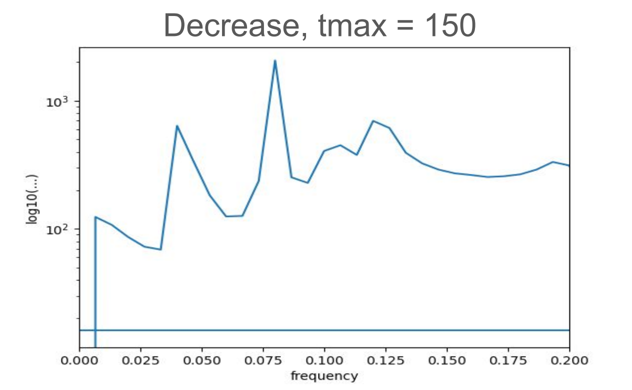

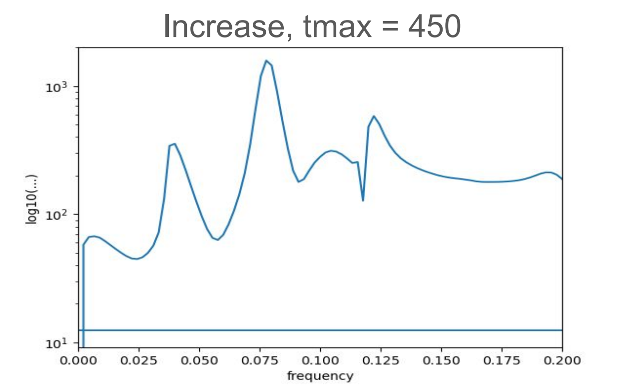

4. Conclusions and Outlook

Summary

- Adding DM cores changes the PSD noticeably
- Can recreate Ellis et al plots using eq. 1-6
- Vary parameters to other reasonable values

Limitations

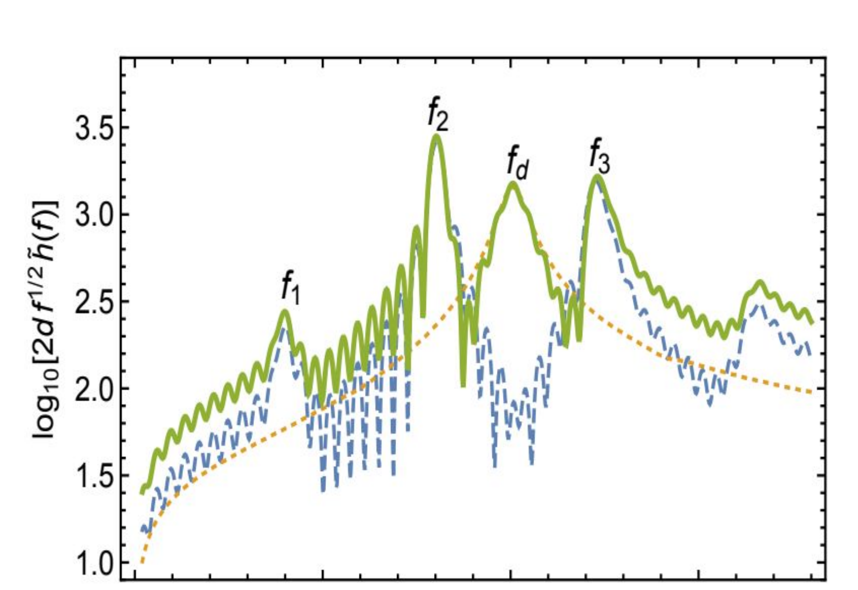

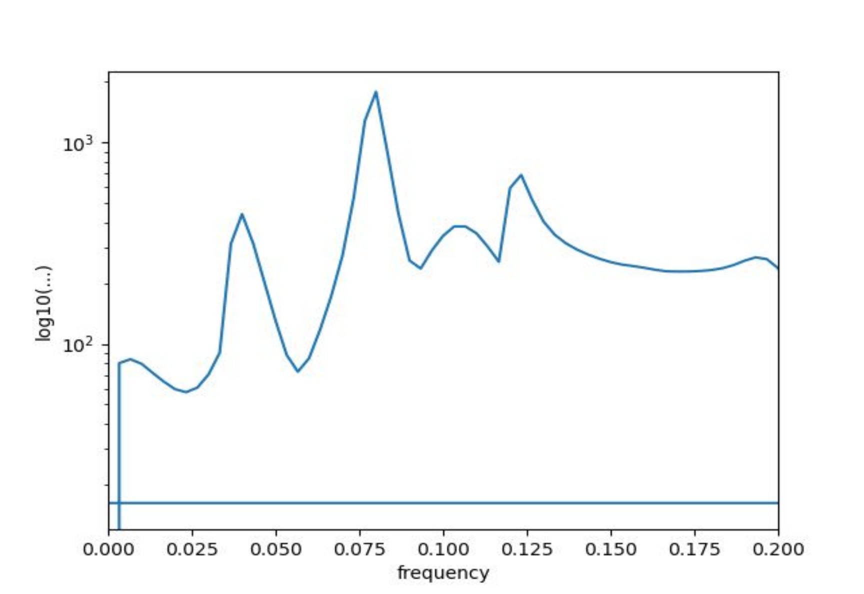

Mini Oscillations not replicated by EXPLORE team

Bibliography

[1] The LIGO Scientific Collaboration, et al. “The Basic Physics of the Binary Black Hole Merger GW150914.” Annalen Der Physik, vol. 529, no. 1–2, Jan. 2017, p. 1600209. arXiv.org, https://doi.org/10.1002/andp.201600209.

[2] Ellis, J., Hektor, A., Hütsi, G., Kannike, K., Marzola, L., Raidal, M., & Vaskonen, V. (2018). Search for Dark Matter Effects on Gravitational Signals from Neutron Star Mergers. *Physics Letters B*, *781*, 607–610. https://doi.org/10.1016/j.physletb.2018.04.048

[3] Takami, K., Rezzolla, L., & Baiotti, L. (2015). Spectral properties of the post-merger gravitational-wave signal from binary neutron stars. *Physical Review D*, *91*(6), 064001. https://doi.org/10.1103/PhysRevD.91.064001